

Single-crystal X-ray diffraction and spectroscopic studies on humboldtine and lindbergite: weak Jahn–Teller effect of Fe²⁺ ion

Takuya Echigo · Mitsuyoshi Kimata

Received: 23 November 2007 / Accepted: 13 April 2008 / Published online: 7 May 2008
© Springer-Verlag 2008

Abstract The single-crystal of humboldtine [Fe²⁺(C₂O₄) · 2H₂O] was first synthesized and the crystal structure has been refined. Single-crystal X-ray diffraction data were collected using an imaging-plate diffractometer system and graphite-monochromatized MoK α radiation. The crystal structure of humboldtine was refined to an agreement index (R1) of 3.22% calculated for 595 unique observed reflections. The mineral crystallizes in the monoclinic system, space group *C2/c*, with unit cell dimensions of *a* = 12.011 (11), *b* = 5.557 (5), *c* = 9.920 (9) Å, β = 128.53 (3)°, *V* = 518.0 (8) Å³, and *Z* = 4. In this crystal structure, the alternation of oxalate anions [(C₂O₄)²⁻] and Fe²⁺ ions forms one-dimensional chain structure parallel to [010]; water molecules (H₂O)⁰ create hydrogen bonds to link the chains, where (H₂O)⁰ is essentially part of the crystal structure. The water molecules with the two lone electron pairs (LEPs) on their oxygen atom are tied obliquely to the chains, because the one lone electron pair is considered to participate in the chemical bonds with Fe²⁺ ions. Humboldtine including hydrogen bonds is isotypic with lindbergite [Mn²⁺(C₂O₄) · 2H₂O]. The donor–acceptor separations of the hydrogen bonds in humboldtine are slightly shorter than those in lindbergite, which suggests that the hydrogen bonds in the former are stronger than those in the latter. The infrared and Raman spectra of single-crystals of humboldtine and

lindbergite confirmed the differences in hydrogen-bond geometry. In addition, Fe²⁺–O stretching band of humboldtine was split and broadened in the observed Raman spectrum, owing to the Jahn–Teller effect of Fe²⁺ ion. These interpretations were also discussed in terms of bond-valence theory.

Keywords Humboldtine · Lindbergite · Crystal structure · Bond-valence theory · Jahn–Teller effect · Hydrogen bond

Introduction

Humboldtine [Fe²⁺(C₂O₄) · 2H₂O] and lindbergite [Mn²⁺(C₂O₄) · 2H₂O] are oxalate dihydrate minerals containing transition metal cations (Gaines et al. 1997; Atencio et al. 2004). The former was found naturally in brown coal (Manasse 1911), lignite (Garavelli 1955) and pegmatite fracture (Matioli et al. 1997) and the latter was discovered in the Lecht Mines, Banffshire, Scotland (Wilson and Jones 1984) and the Lavra da Boca Rica granite pegmatite (Atencio et al. 2004); these two minerals are considered to occur as secondary minerals.

Many structural analyses of humboldtine and lindbergite were reported (humboldtine: Mazzi and Garavelli 1957, 1959; Caric 1959; Deyrieux and Peneloux 1969; Śledzińska et al. 1986, lindbergite: Deyrieux et al. 1973; Śledzińska et al. 1987). However, considerable difficulties are faced in preparing single-crystals of the oxalate complexes containing transition metals (Kitagawa et al. 1995) because stacking faults commonly occur in their crystal structures (Pezerat et al. 1968; Lagier et al. 1969; Dubernat and Pezerat 1974). Hence the structure refinement of humboldtine based on the single-crystal X-ray diffraction data has not

T. Echigo · M. Kimata
Earth Evolution Sciences, Life and Environmental Sciences,
University of Tsukuba, Tennoudai 1-1-1,
Tsukuba 305-8572, Ibaraki, Japan

Present Address:

T. Echigo (✉)
Japan International Research Center for Agricultural Sciences,
Ohwashi 1-1, Tsukuba 305-8686, Ibaraki, Japan
e-mail: echigo@jircas.affrc.go.jp

been successfully made, although that of lindbergite has been recently done by Soleimannejad et al. (2007). Detailed crystal-chemical analyses using single-crystals may provide structural insight into the oxalate minerals.

Here, we present the result of X-ray diffraction structure analysis of the synthetic single-crystals of humboldtine. In addition, micro-infrared absorption and micro-Raman scattering analyses using single-crystals of humboldtine and lindbergite were performed to compare with each other in terms of hydrogen bond geometries in their crystal structures. Their crystal chemical characteristics including Jahn–Teller effect of Fe^{2+} ion (Benarafa et al. 2000; Fritsch et al. 2004), hydrogen bond geometries, and the role of lone electron pairs (LEPs) of water molecules will come up for detailed discussion.

Experimental

Preparation of single-crystals of humboldtine and lindbergite

Single-crystals of humboldtine and lindbergite were synthesized by reactions of oxalic acid ester with iron sulfate hexahydrate ($\text{Fe}^{2+}\text{SO}_4 \cdot 6\text{H}_2\text{O}$) and manganese chloride tetrahydrate ($\text{Mn}^{2+}\text{Cl}_2 \cdot 4\text{H}_2\text{O}$), respectively. The preparation of humboldtine was carried out under hydrothermal conditions in Teflon-lined stainless steel autoclaves with autogeneous pressure (ca. 0.5 MPa). The mixture of aqueous solution of diethyl oxalate ($\text{C}_6\text{H}_{10}\text{O}_4$) with an aqueous solution of iron sulfate hexahydrate in a stoichiometric proportion was prepared. The Teflon vessel was filled to 40% of its inner volume by the mixture solution and was then heated to 393 K, kept at this temperature for 72 h, and slowly cooled to room temperature overnight. Consequently, yellow prism crystals of humboldtine, with maximum length of approximately 5 mm, were obtained. On the other hand, lindbergite crystals were synthesized by reaction of aqueous solution of dimethyl oxalate ($\text{C}_4\text{H}_6\text{O}_4$) with an aqueous solution of manganese chloride tetrahydrate in a stoichiometric proportion at room temperature (296 K). The reaction was induced in a glass cup for 14 weeks and the products deposited in the bottom of the cup were colorless and single-crystals of lindbergite up to 2-mm long. Both of the precipitates were washed with distilled water, filtered and dried. Each product was confirmed by X-ray powder diffraction analysis to consist only of humboldtine and lindbergite, respectively.

Single-crystal X-ray crystal structure analysis of humboldtine

Single-crystal of humboldtine was chosen under a stereomicroscope and a polarizing microscope, and then single-

crystal X-ray diffraction dataset was collected with an imaging-plate diffractometer system (Rigaku RAXIS-RAPID, $\text{MoK}\alpha$ radiation, graphite monochromator). Intensity data were corrected for Lorenz and polarization effects. Empirical absorption correction (Higashi 1995) was used. Selected crystallographic and experimental data together with the refinement details are given in Table 1. Structure solution and refinement have been carried out by direct method (SIR97: Altomare et al. 1999). Positions of hydrogen atoms were determined on a 3-D difference-Fourier map (Beurskens et al. 1999) around the associated oxygen atoms under the restrictions on O–H bond distances ($0.98 \pm 0.02 \text{ \AA}$). The full-matrix least-squares refinements on F^2 were done using the SHELXL-97 program (Sheldrick 1997) with anisotropic displacement parameters for non-hydrogen atoms and isotropic ones for hydrogen atoms.

Bond-valence analysis

Bond-valence analyses were performed for humboldtine and lindbergite; the former analysis was made based on the bond lengths obtained from the present structure refinement and the latter was according to Soleimannejad et al. (2007). The calculations were carried out with the program VALENCE (Brown 1996). However, bond-valences of hydrogen bonds

Table 1 Summarized crystal data and details of refinement parameters

Chemical formula	$\text{Fe}^{2+} (\text{C}_2\text{O}_4) \cdot 2\text{H}_2\text{O}$
Crystal dimensions	$0.15 \times 0.05 \times 0.05 \text{ mm}$
Temperature	293 K
Lattice parameters	
<i>a</i>	12.011 (11) \AA
<i>b</i>	5.557 (5) \AA
<i>c</i>	9.920 (9) \AA
β	128.53 (3) $^\circ$
<i>V</i>	518.0 (8) \AA^3
<i>Z</i>	4
<i>D</i> _{calc}	2.307 g/cm^3
Space group	<i>C2/c</i>
<i>F</i> ₀₀₀	360.00
μ ($\text{MoK}\alpha$)	28.624 cm^{-1}
Measured reflections	2,405
Independent reflections, <i>R</i> _{int}	595, 3.2%
<i>R</i> ₁ , <i>wR</i> ₂ (All data)	3.74%, 9.31%
Observed reflections [<i>I</i> _o > 2σ(<i>I</i> _o)]	595
Parameters used in the refinement	51
Reflection/parameter ratio	11.67
<i>R</i> ₁ [<i>I</i> _o > 2σ(<i>I</i> _o)]	3.22%
Goodness of fit indicator	1.387
Max. peak in final diff. map	0.64 e/\AA^3
Min. peak in final diff. map	−0.66 e/\AA^3

Table 2 Atomic coordinates and displacement parameters (\AA^2) for humboldtine

Atom	<i>x</i>	<i>y</i>	<i>z</i>	<i>B</i> _{eq}	occ.	<i>U</i> ₁₁	<i>U</i> ₂₂	<i>U</i> ₃₃	<i>U</i> ₁₂	<i>U</i> ₁₃	<i>U</i> ₂₃
Fe	0	0.1704 (15)	1/4	1.44 (2)	1/2	0.0248 (4)	0.0097 (3)	0.0162 (4)	0	0.0107 (3)	0
C	0.0499 (3)	0.6684 (7)	0.3511 (4)	1.27 (5)	1	0.0255 (14)	0.0153 (14)	0.0133 (12)	0.0018 (12)	0.0078 (11)	0.0013 (11)
O(1)	0.0848 (3)	0.4694 (5)	0.4227 (3)	1.66 (5)	1	0.0330 (16)	0.0126 (14)	0.0148 (12)	−0.0010 (12)	0.0111 (12)	−0.0018 (11)
O(2)	0.0863 (3)	0.8716 (5)	0.4236 (3)	1.80 (5)	1	0.0272 (15)	0.0336 (17)	0.0183 (13)	0.0050 (15)	0.0126 (12)	0.0036 (14)
O(3)	0.1797 (3)	0.1777 (6)	0.2573 (3)	2.17 (5)	1	0.0172 (17)	0.0152 (17)	0.0137 (17)	−0.0001 (16)	0.0086 (15)	−0.0003 (16)
H(1)	0.263 (5)	0.091 (12)	0.349 (7)	8.2 (23)	1						
H(2)	0.167 (5)	0.130 (10)	0.156 (4)	3.5 (12)	1						

were assigned according to Hawthorne (1992a, b; 1997), since the O–H distances are restricted as mentioned above and bond-valence calculations depend primarily upon the corresponding bond-distances (Brown 1981, 2002).

Infrared and Raman spectroscopic analyses

Single-crystal infrared spectra were obtained using a Janssen-type micro-FTIR spectrometer (JASCO corp.). Single-crystals of humboldtine and lindbergite (~5- μm thick) were chosen under a stereomicroscope and placed on a KBr plate. The spectra were measured in the region of 4,000–650 cm^{-1} , with 1 cm^{-1} resolution and 400 scans were performed at room temperature in air.

Raman scattering measurements were carried out using a micro-Raman spectrometer (Photon-Design Mars) equipped with a monochromator (JOBIN YVON HR-320) and a CCD detector (ANDOR DU-401). Approximately 100 mW of power at 514.5 nm wavelength from an Ar

laser (Spectra Physics Stabilite 2017) was used to excite the samples. The measurements were made in air at room temperature.

Results

Structure description

The crystal structure of humboldtine was finally refined to $R = 3.22\%$ for the 595 unique observed [$I_o > 2\sigma(I_o)$] reflections (Table 1). The final positional parameters and displacement parameters are given in Table 2. Selected bond distances, angles, and hydrogen bonds geometry are shown in Table 3. Interatomic distances listed in Table 3 agree closely with the previous result obtained from neutron powder diffraction method (Śledzińska et al. 1986), though the present structure analysis is more convergent. Bond-valence distribution is shown in Table 4.

Table 3 Selected bond lengths (\AA) and angles ($^\circ$) for humboldtine

Iron polyhedron		Oxalate anion	
Fe–O(1)	2.135 (2) \AA	C–O(1)	1.238 (4) \AA
Fe–O(2)	2.139 (2)	C–O(2)	1.261 (4)
Fe–O(3)	2.114 (4)	Mean	1.250
Mean	2.129	C–C	1.570 (4) \AA
Polyhedral volume ^a	12.59 \AA^3		
BLD value ^b	0.48%		
		O(1)–C–C	116.7 (3) $^\circ$
Water molecule		O(2)–C–C	116.5 (3)
O(3)–H(1)	0.96 (5) \AA	Mean	116.6
O(3)–H(2)	0.95 (5) \AA	O(1)–C–O(2)	126.8 (3) $^\circ$
H(1)–O(3)–H(2)	104 (2) $^\circ$		
Hydrogen bonds			
H(1)···O(1)	1.85 (4) \AA	H(2)···O(2)	1.87 (4) \AA
O(3)···O(1)	2.749 (3) \AA	O(3)···O(2)	2.769 (5) \AA
O(3)–H(1)···O(1)	154 (6) $^\circ$	O(3)–H(2)···O(2)	157 (5) $^\circ$

^a Calculated using CrystalMaker program (CrystalMaker Software 2007)

^b BLD(bond length distortion) = $\frac{100}{n} \sum_{i=1}^n [\{(X-O)_i - \langle X-O \rangle\} / \langle X-O \rangle]$, where n = number of bonds, $(X-O)_i$ = central cation–oxygen length and $\langle X-O \rangle$ = average cation–oxygen bond length (Renner and Lehmann 1986)

Table 4 Bond-valences (v.u.) and their sums for humboldtine

	Fe	C	H(1) ^a	H(2) ^a	Sum
O(1)	0.338 ^{x2↓}	1.516	0.179		2.034
O(2)	0.335 ^{x2↓}	1.425		0.179	1.939
O(3)	0.358 ^{x2↓}		0.821	0.821	2.000
C		0.973			
Sum	2.062	3.914	1.000	1.000	

^a Bond-valences of hydrogen bonds were determined by assuming that the valence sum is 1.000 v.u.

As seen in Fig. 1, the three-dimensional structure of humboldtine consists of linear infinite chains along [010], linked together by the hydrogen bonds. The hydrogen bonds are formed between the oxygen atoms of the water molecules (O3) and those of the oxalate ions (O1 and O2) belonging to adjacent chains. In the oxalate minerals, the alternation of oxalate anions $[(C_2O_4)^{2-}]$ and Fe^{2+} ions creates the 1D chain structure parallel to [010]; water molecules $(H_2O)^0$ between the chains form hydrogen bonds, with which they are linked together (Fig. 1). Therefore $(H_2O)^0$ is essentially part of the crystal structure. Additionally, the water molecules are tied at a slight tilt to the chains (Fig. 1). Humboldtine including hydrogen bonds is isotypic with lindbergite reported by Soleimannejad et al. (2007).

Bond-valence calculations

Calculations of bond-valence for humboldtine and lindbergite were carried out, and their results are given in Tables 4 and 5, respectively. The sums of the bond-

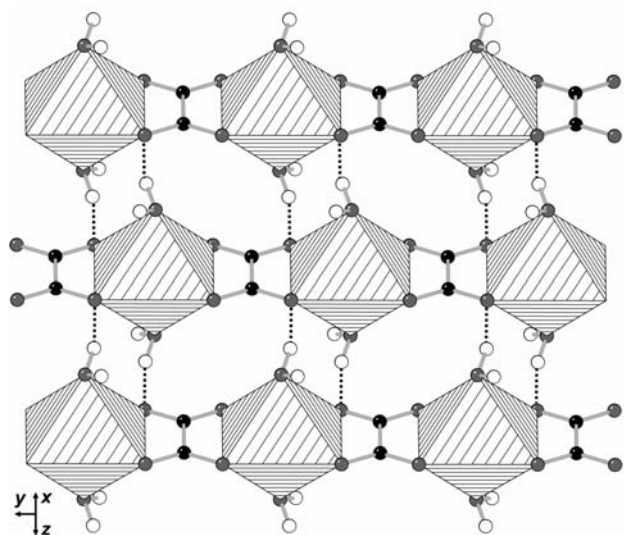


Fig. 1 Crystal structure of humboldtine. Cation polyhedra are striped, carbon atoms are shown in black, oxygen in pale gray and hydrogen atoms are white; dotted lines represent hydrogen bonds

Table 5 Bond-valences (v.u.) and their sums for lindbergite

	Mn	C	H(1) ^a	H(2) ^a	Sum
O(1)	0.355 ^{x2↓}	1.462	0.169		1.986
O(2)	0.344 ^{x2↓}	1.442		0.169	1.955
O(3)	0.338 ^{x2↓}		0.831	0.831	2.000
C		0.981			
Sum	2.075	3.885	1.000	1.000	

Bond distances are taken from Soleimannejad et al. (2007)

^a Bond-valences of hydrogen bonds were determined by assuming that the valence sum is 1.000 v.u.

valences around the iron atom and manganese atom are 2.062 and 2.075 valence unit (v.u.), respectively, which are in good agreement with the expected value (2.000) for each atom. Similarly, the sums of the valences around the Fe-coordinated oxygen atoms and the Mn-coordinated oxygen atoms lie in the range 1.939–2.034 (average value, 1.991 v.u.) and 1.955–2.000 (average value, 1.980 v.u.), respectively. Both of them are also in accordance with the expected value (2.000) for oxygen atom. Calculations of such bond-valences show that the valence sum rule (Brown 1981, 2002) is obeyed not only within the Fe-polyhedra and Mn-polyhedra, but also around the polyhedra. The bond-valence analyses ensured the reliability of these two crystal structures; the crystal-chemical relationship between humboldtine and lindbergite will be discussed in detail later.

Infrared spectroscopy

The IR spectra for humboldtine and lindbergite are shown in Fig. 2. The former is closely parallel to the latter throughout the range of their observed IR spectra. In the O–H stretching frequency regions of humboldtine and lindbergite ($2,600\text{--}3,400\text{ cm}^{-1}$; Nakamoto 1997), each prominent band is present at $3,300\text{ cm}^{-1}$ (Fig. 2a) and $3,312\text{ cm}^{-1}$ (Fig. 2b), respectively. Both of the bands have six shoulders; the former shoulders were observed at 3,167, 3,104, 2,978, 2,944, 2,820 and $2,773\text{ cm}^{-1}$ (Fig. 2a) and the latter ones at 3,155, 3,089, 2,977, 2,935, 2,820 and $2,770\text{ cm}^{-1}$ (Fig. 2b). O–H bending bands (Nakamoto 1997) are centered at $1,656\text{ cm}^{-1}$ in the spectrum of humboldtine (Fig. 2a) and at $1,655\text{ cm}^{-1}$ in that of lindbergite (Fig. 2b). The shoulder bands observed at $1,600\text{ cm}^{-1}$ for humboldtine (Fig. 2a) and $1,604\text{ cm}^{-1}$ for lindbergite (Fig. 2b) are assigned to O–C–O antisymmetric stretching bands (Silverstein et al. 1991). In addition, O–C–O symmetric stretching bands (Silverstein et al. 1991) are recognized at $1,357$ and $1,313\text{ cm}^{-1}$ in the spectrum of humboldtine (Fig. 2a) and at $1,359$ and $1,310\text{ cm}^{-1}$ in that of lindbergite (Fig. 2b).

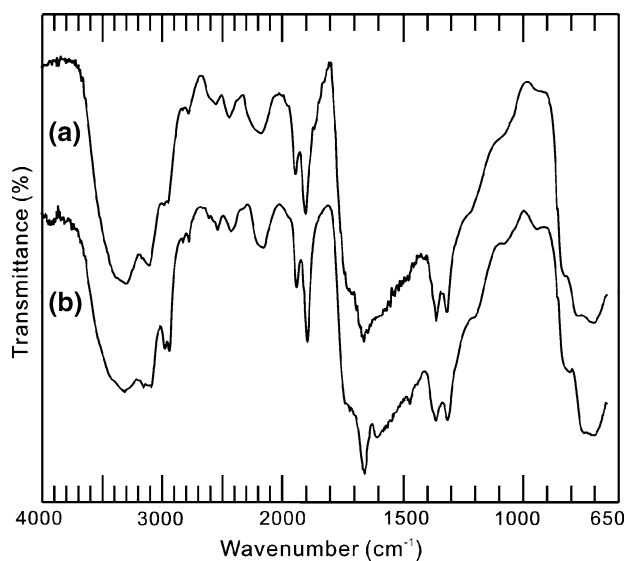


Fig. 2 Micro-infrared spectra of **a** humboldtine and **b** lindbergite

Raman spectroscopy

The Raman spectra for humboldtine and lindbergite are shown in Figs. 3 and 4. The former is closely parallel to both the latter and the natural sample reported by Frost (2004) throughout a range of the observed spectra. In the O–H stretching frequency regions of humboldtine and lindbergite (2,900–3,500 cm^{-1} ; Smith and Dent 2005), the broad band centered at 3,316 cm^{-1} is present in the former (Fig. 3a) and it is at 3,326 cm^{-1} in the latter (Fig. 3b). Prominent C–O stretching bands (Frost 2004) are observed at 1,463 cm^{-1} for humboldtine (Fig. 3a) and 1,469 cm^{-1} for lindbergite (Fig. 3b), respectively. The sharp bands centered at 585 and 915 cm^{-1} in the spectrum of humboldtine (Fig. 4a) are assigned to water libration and O–C–

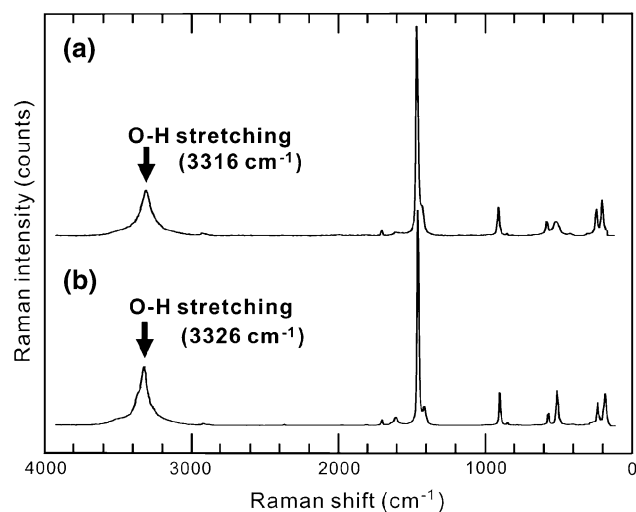


Fig. 3 Micro-Raman spectra of **a** humboldtine and **b** lindbergite

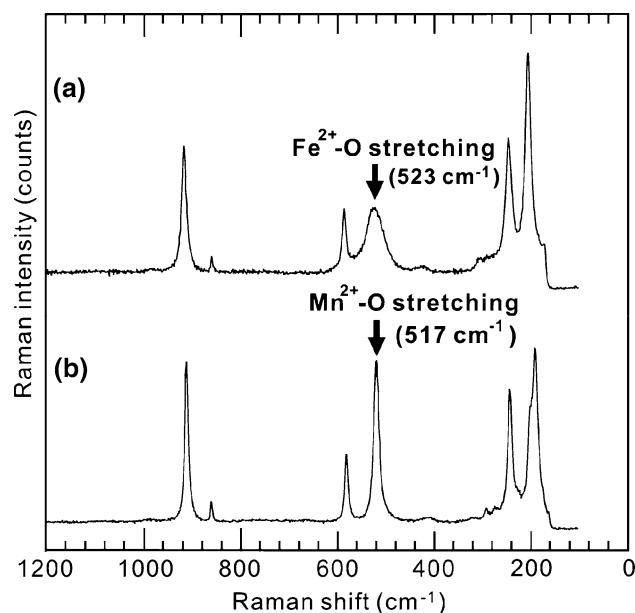


Fig. 4 Micro-Raman spectra of the 100–1,200 cm^{-1} region of **a** humboldtine and **b** lindbergite: the former Fe^{2+} –O stretching band (523 cm^{-1}) is broader and less intense than the latter Mn^{2+} –O one (517 cm^{-1}) owing to the Jahn–Teller effect of Fe^{2+} ion

O bending modes (Frost 2004), respectively. In the spectrum of lindbergite (Fig. 4b), the equivalent bands are located at 579 and 908 cm^{-1} , respectively. In addition, the band doublet at 204/245 cm^{-1} in the spectrum of humboldtine (Fig. 4a) is attributed to the lattice mode (Nakamoto 1997). The same doublet was observed at 198/240 cm^{-1} in the spectrum of humboldtine (Fig. 4b). Figure 4 shows that the Fe^{2+} –O stretching band centered at 523 cm^{-1} is significantly broader and less intense than the Mn^{2+} –O stretching band centered at 517 cm^{-1} .

Discussion

Octahedral distortions

The coordination environment of Fe^{2+} in humboldtine is a distorted octahedron where the two metal–water bonds (Fe–O3) are shorter than the other four metal–oxalate bonds (Fe–O1 and Fe–O2) (Fig. 5). On the other hand, the Mn^{2+} –octahedron in lindbergite (Soleimannejad et al. 2007) is also slightly distorted; the two metal–water bonds (Mn–O3) are longer than the other four metal–oxalate bonds (Mn–O1 and Mn–O2) (Fig. 5). Calculated values of bond length distortion (BLD; Renner and Lehmann 1986) for the Fe- and Mn-octahedra are 0.48 and 0.28%, respectively. Note that the former octahedron is horizontally elongated though the latter is horizontally contracted and the former BLD value is larger than the latter. The difference in geometry between

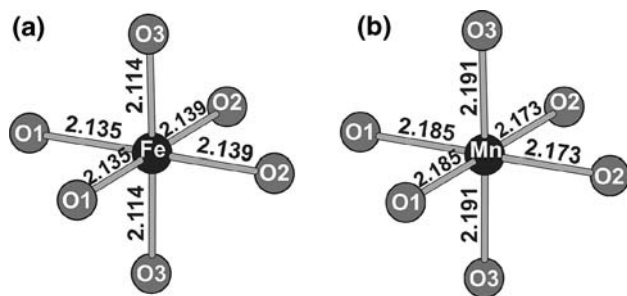


Fig. 5 Comparison between **a** FeO₆-octahedron in humboldtine and **b** MnO₆-octahedron in lindbergite (Soleimannejad et al. 2007). Observed bond distances (Å) are shown

these Fe- and Mn-octahedra may result from the weak Jahn–Teller effect of Fe²⁺ ion (Benarafa et al. 2000; Fritsch et al. 2004). Since Fe²⁺ ion has asymmetric *t*_{2g} configuration of electrons (Burns 1993; Moore 2004), the orbital group may cause the Jahn–Teller effect (Jahn and Teller 1937; Orgel and Dunitz 1957; Dunitz and Orgel 1957).

The horizontal distortion of Fe²⁺O₆ polyhedra in humboldtine may stem from the geometrical coordination between Fe²⁺ ion and oxalate anion. Figure 6 shows the geometry of cation-anion coordination in the chain structures along [010]. Both of the cation polyhedra in the present minerals are significantly elongated along [010]. Mn²⁺O₆ polyhedra are more elongated along the main axis (O3–O3) than Fe²⁺O₆ polyhedra since the ionic radius of the former (0.83 Å: Shannon 1976) is larger than that of the latter (0.78 Å: Shannon 1976). On the other hand, the geometries of oxalate anions show little difference between their structures, which demonstrates that the oxalate anion is more rigid than the cation polyhedra. The rigidity of oxalate anion gives rise to significantly narrow bond angles called “bite-angle” defined as O–M–O angle where the oxygen atoms belong to the same oxalate anion (Stiefel and

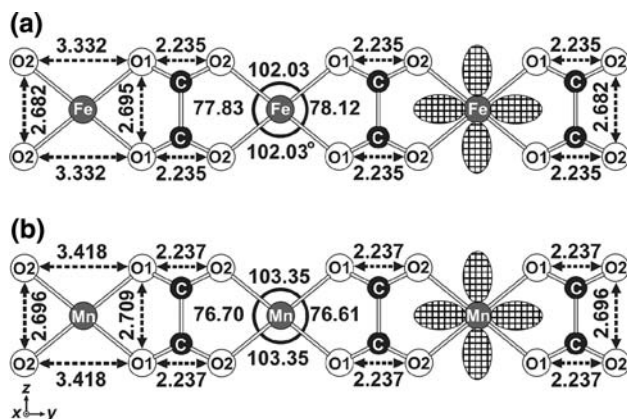


Fig. 6 Comparison between the geometries of the chain structures in **a** humboldtine and **b** lindbergite (Soleimannejad et al. 2007). Observed bond distances (Å) and angles (°) are shown; the *d*_{xy} orbitals are cross-hatched

Brown 1972). The bite-angles having values far away from the ideal octahedral ones (90°) exert a crystal-chemical influence on the oxalate complexes containing transition-metals (Calatayud et al. 2000; Castillo et al. 2001).

Figure 6 shows the shape of *d*_{xy} orbitals of the corresponding cations in the chain structures. The *d*_{xy} orbitals point to the regions where there is no ligand. However, small repulsion due to the narrow bite-angles in humboldtine (77.83° and 78.12°) may occur between the orbitals and ligands (oxygen atoms belonging to oxalate anions). Thus the repulsion induced by the narrow bite-angles causes the Fe²⁺O₆ polyhedra to be horizontally elongated. The Mn²⁺O₆ polyhedra are less distorted than Fe²⁺O₆ polyhedra in terms of BLD values as mentioned above, while the bite-angles in lindbergite (76.61° and 76.70°: Soleimannejad et al. 2007) are narrower than those (77.83° and 78.12°) in humboldtine (Fig. 6). These differences can be explained both by the fact that high-spin Mn²⁺ ion causes no Jahn–Teller effect (Jahn and Teller 1937; Orgel and Dunitz 1957; Dunitz and Orgel 1957) and by the interpretation that the octahedral distortion in humboldtine is caused by asymmetric *t*_{2g} configuration of electrons.

Bond-valence calculations revealed that the elongated Fe–O1 and Fe–O2 bonds contribute to less bond-valence than the corresponding Mn–O1 and Mn–O2 in lindbergite (Tables 4 and 5). However the short Fe–O3 bond distance supplies its bond-valence to satisfy the bond-valence requirement from central Fe²⁺ ion (Table 4). As a result, valence sum of each atom in humboldtine is nearly identical with that in lindbergite (Tables 4 and 5), which suggests that the degeneracy of *t*_{2g} orbitals is removed and the energy level of *d*_{xy} orbital became more stable.

Spectroscopic evidences for the Jahn–Teller effect were also provided by the present Raman spectra. The Fe²⁺–O stretching band in humboldtine is significantly broader and less intense than the Mn²⁺–O one in lindbergite as already explained (Fig. 4). Both the broadening and lowering the intensity of the Fe²⁺–O band may arise from the Jahn–Teller effect of Fe²⁺ ion (Cotton and Meyers 1960; Bersuker and Vekhter 1962). On the other hand, the metal-oxygen stretching frequencies generally decrease as the mass of the metal increases (Nakamoto 1997). However, humboldtine has higher metal-oxygen stretching frequency (523 cm^{−1}) due to the Jahn–Teller effect of the Fe²⁺ ion than does lindbergite (517 cm^{−1}), as previously reported by Adams and Morris (1968).

Hydrogen bonds

In the geometries of hydrogen bonds of humboldtine (Table 3), the distances between donor oxygen (O_D) and acceptor (O_A) oxygen are 2.749 and 2.769 Å (average value, 2.759 Å). In those of lindbergite (Soleimannejad

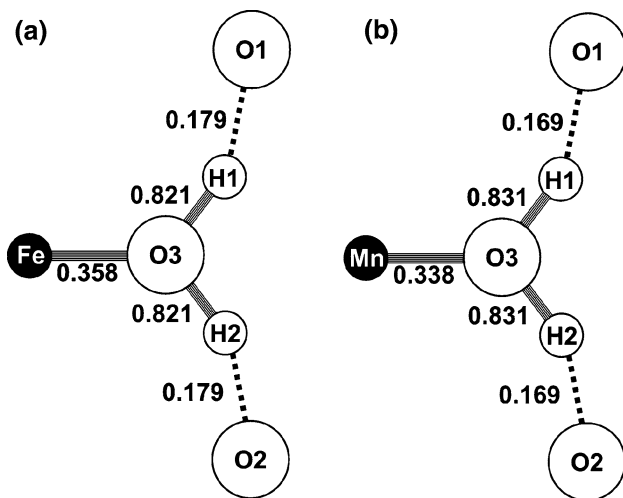


Fig. 7 Schematic representations of the bond-valence structures of hydrogen bonds in **a** humboldtine and **b** lindbergite; calculated bond-valences (v.u.) are shown

et al. 2007), the $O_D \cdots O_A$ distances are 2.769 and 2.751 Å (average value, 2.758 Å). Since the $O_D \cdots O_A$ distances of humboldtine are slightly shorter than those of lindbergite, the former hydrogen bonds are found to be slightly stronger than the latter.

Bond-valence distributions of the hydrogen bonds are schematically represented in Fig. 7, which shows that the Fe–O3 bond contributes a bond-valence of 0.358 v.u. to the oxygen and the remaining 1.642 v.u. is supplied by its two attendant hydrogen atoms. Each hydrogen atom supplies a bond-valence of $1.642/2 = 0.821$ v.u. to the oxygen (O3), then the remaining $1.000 - 0.821 = 0.179$ v.u. is provided by the weak hydrogen bonds linking hydrogens of water molecules to O1 of their adjacent chains (Fig. 7a). On the other hand, the Mn–O3 bond contributes its bond-valence (0.338 v.u.) to the oxygen (O3) and the remaining 1.662 v.u. is supplied by the two attendant hydrogen atoms (Fig. 7b). Each hydrogen atom contributes a bond-valence of $1.662/2 = 0.831$ v.u. to the oxygen (O3) and hence the remaining $1.000 - 0.831 = 0.169$ v.u. is provided by the weak hydrogen bonds linking hydrogens of water molecules to O1 of their adjacent chains. The bond-valences of hydrogen bonds (0.179 v.u.) attracting the Fe^{2+} -oxalate chains are higher than those (0.169 v.u.) attracting the Mn^{2+} -oxalate chains, which is consistent with the conclusion derived from the present crystal structure refinements: hydrogen bonds in humboldtine are slightly stronger than those in lindbergite.

In addition to theoretical calculations (Bellamy and Owen 1969), empirical correlation diagrams showed conclusively that the wavenumber of O–H stretching band decreases considerably with increasing strength (decreasing length) of the hydrogen bond (Nakamoto et al. 1955;

Novak 1974; Mikenda 1986; Libowitzky 1999). In the observed FTIR spectra, the wavenumbers of their O–H stretching bands are observed to be $3,300\text{ cm}^{-1}$ for humboldtine and $3,312\text{ cm}^{-1}$ for lindbergite. These results show that both their bands may be regarded as due to weak hydrogen bonds (Libowitzky 1999) and that the former hydrogen bonds are slightly stronger than the latter. The present Raman spectra also indicate that humboldtine has stronger hydrogen bonds, with the present observation that the wavenumbers of O–H stretching band are centered at 3,316 and $3,326\text{ cm}^{-1}$ for humboldtine and lindbergite, respectively. These spectroscopic data are quite consistent with the result of the crystal structure refinements discussed above: the $O_D \cdots O_A$ distances of humboldtine are shorter than those of lindbergite.

Tilting of water molecules

Consider the arrangements of water molecules in the crystal structures of humboldtine and lindbergite, both of which are isotopic with each other (Fig. 1); these water molecules are obliquely tied to the chains consisting of metal cations and oxalate anions. The schematic representation of the electronic structure is shown in Fig. 8a, where both metal cation and oxalate anion constitute one-dimensional chains linked by ionic bonds ($-M^{2+}-ox^{2-}-M^{2+}-ox^{2-}-M^{2+}$; $M = Fe$ or Mn , $ox = oxalate$). The water molecule donates one of two lone electron pairs (LEPs) to metal cation to form coordinate covalent bond (Fig. 8a). Thus, one of two LEPs of the water molecule is shared with the corresponding cation and served as chemical bonding. On the other hand, the remaining LEP exists as one non-bonding electron pair (Fig. 8a). The remaining LEP may impose spatial requirement from the

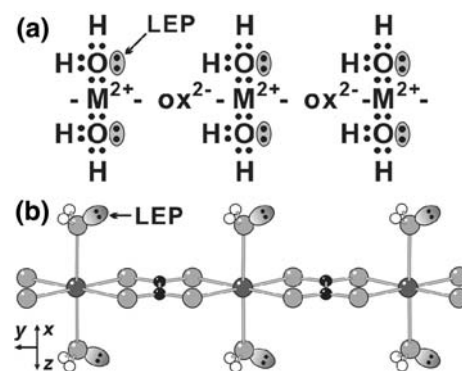


Fig. 8 **a** Schematic representation of electronic structure ($M = Fe$: humboldtine, Mn : lindbergite; ox : oxalate ion) of the chain structures in the oxalate minerals. **b** The three-dimensional structures of the chains. Metal (Fe/Mn) atoms are shown in dark gray, oxygen in pale gray, carbon in black, and hydrogen in white. The water molecules tied to the chains are tilted by the spatial requirements of the lone electron pairs (LEPs)

perspective of the Valence Shell Electron Pair Repulsion (VSEPR) model (Gillespie 1971); each pair of electrons in the valence shell is localized in a way that minimizes the repulsion between them. Bonding electron pairs point towards the atoms they bond, but the non-bonding LEPs point to a region where there is no atom (Gillespie and Hargittai 1991) and hence the water molecules are tied at a slight tilt to the chains (Fig. 8b).

Acknowledgments This investigation was supported by Research Fellowships of the Japan Society for the Promotion of Science for Young Scientists (project no. 17-7332). Single-crystal X-ray data collection was performed at the Chemical Analysis Division, Research Facility Center for Science and Technology, University of Tsukuba. Helpful comments by Dr. Daniel Atencio and an anonymous reviewer led to improvements in the manuscript. We are indebted to Dr. Milan Rieder for handling of this manuscript.

References

- Adams DM, Morris DM (1968) Vibrational spectra of halides and complex halides. Part IV. Some tetrahalogenoallates and the effects of d-electronic structure on the frequencies of hexachlorometallates. *J Chem Soc A* 20:694–695
- Altomare A, Burla M, Camalli M, Casciarano G, Giacovazzo C, Guagliardi A, Moliterni A, Polidori G, Spagna R (1999) SIR97: a new tool for crystal structure determination and refinement. *J Appl Crystallogr* 32:115–119
- Atencio D, Coutinho JMV, Graesser S, Matioli PA, Menezes F, Luiz AD (2004) Lindbergite, a new Mn oxalate dihydrate from Boca Rica mine, Galileia, Minas Gerais, Brazil, and other occurrences. *Am Mineral* 89:1087–1091
- Bellamy LJ, Owen AJ (1969) A simple relationship between the infrared stretching frequencies and the hydrogen bond distances in crystals. *Spectrochim Acta* A25:329–333
- Benarafa A, Kacimi M, Gharbage S, Millet JMM, Ziyad M (2000) Structural and spectroscopic properties of calcium-iron $\text{Ca}_9\text{Fe}(\text{PO}_4)_7$ phosphate. *Mater Res Bull* 35:2047–2055
- Bersuker IB, Vekhter BG (1962) Splitting of infrared absorption and Raman spectra in octahedral complexes of transitional metals as a result of internal asymmetry. *Izv Akad Nauk Mold* 10:11–17
- Beurskens PT, Admirala G, Beurskens G, Bosman WP, de Gelder R, Israel R, Smits JMM (1999) The DIRDIF-99 program system. Technical Report of the Crystallography Laboratory, University of Nijmegen
- Brown ID (1981) The bond-valence method: an empirical approach to chemical structure and bonding. In: O’Keeffe M, Navrotsky A (eds) *Structure and bonding in crystals II*. Academic Press, New York, pp 1–30
- Brown ID (1996) VALENCE: a program for calculating bond valences. *J Appl Crystallogr* 29:479–480
- Brown ID (2002) The chemical bond in inorganic chemistry, the bond valence model. IUCr monographs on crystallography 12. International Union of Crystallography, Oxford Science Publications, Oxford
- Burns RG (1993) Mineralogical applications of crystal field theory, 2nd edn. Cambridge University Press, Cambridge
- Calatayud ML, Castro I, Sletten J, Lloret F, Julve M (2000) Syntheses, crystal structures and magnetic properties of chromato-, sulfato-, and oxalato-bridged dinuclear copper(II) complexes. *Inorg Chim Acta* 300–302:846–854
- Caric S (1959) The structure of humboldtine ($\text{FeC}_2\text{O}_4 \cdot 2\text{H}_2\text{O}$). *Bull Soc Fr Miner Cristallogr* 82:50–56
- Castillo O, Luque A, Julve M, Lloret F, Román P (2001) One-dimensional oxalato-bridged copper(II) complexes with 3-hydroxypyridine and 2-amino-4-methylpyridine. *Inorg Chim Acta* 315:9–17
- Cotton FA, Meyers MD (1960) Magnetic and spectral properties of the spin-free $3d^6$ systems iron(II) and cobalt(III) in cobalt(III) hexafluoride ion: probable observation of dynamic Jahn–Teller effects. *J Amer Chem Soc* 82:5023–5026
- CrystalMaker Software (2007) CrystalMaker—CrystalMaker Software. Bicester, Oxfordshire
- Deyrieux R, Peneloux A (1969) Divalent metal oxalates. I. Crystal structure of two allotropic forms of dihydrated ferrous oxalate. *Bull Soc Chim Fr* 8:2675–2681
- Deyrieux R, Berro C, Peneloux A (1973) Oxalates of some divalent metals. III. Crystal structure of dihydrated manganese, cobalt, nickel, and zinc oxalates. Polymorphism of dihydrated cobalt and nickel oxalates. *Bull Soc Chim Fr* 1:25–34
- Dubernat J, Pezerat H (1974) Stacking faults in the dihydrated oxalates of divalent metals of the magnesium series (magnesium, manganese, iron, cobalt, nickel, zinc). *J Appl Crystallogr* 7:387–393
- Dunitz JD, Orgel LE (1957) Electronic properties of transition-metal oxide I: distortions from cubic symmetry. *J Phys Chem Solids* 3:20–29
- Fritsch V, Hemberger J, Büttgen N, Scheidt EW, Krug von Nidda HA, Loidol A, Tsurkan V (2004) Spin and orbital frustration in MnSc_2S_4 and FeSc_2S_4 . *Phys Rev Lett* 92(11):116401-1–116401-4
- Frost RL (2004) Raman spectroscopy of natural oxalates. *Anal Chim Acta* 517:207–214
- Gaines RV, Skinner HCW, Foord EE, Mason B, Rosenzweig A (1997) Dana’s new mineralogy: the system of mineralogy of James Dwight Dana and Edward Salisbury Dana, 8th edn. John Wiley, New York
- Garavelli C (1955) Discovery of oxalite among the secondary minerals of the Capo Calamita layer. *Rend Soc Miner Ital* 11:176–181
- Gillespie RJ (1971) *Molecular geometry*. Van Nostrand Reinhold, New York
- Gillespie RJ, Hargittai I (1991) *The VSEPR model of molecular geometry*. Allyn and Bacon, Boston
- Hawthorne FC (1992a) The role of OH and H_2O in oxide and oxysalt minerals. *Z Kristallogr* 201:183–206
- Hawthorne FC (1992b) Bond topology, bond valence and structure stability. In: Price GD, Ross NL (eds) *The stability of minerals*. Wiley series in advances in environmental science and technology 29, Chapman and Hall, London, pp 25–87
- Hawthorne FC (1997) Structural aspects of oxide and oxysalt minerals. In: Merlino S (ed) *EMU notes in mineralogy*, vol. 1: modular aspects of minerals, Eötvös University Press, Budapest, pp 373–429
- Higashi T (1995) Abscor—empirical absorption correction based on Fourier series approximation. Rigaku Corporation, Tokyo
- Jahn HA, Teller E (1937) Stability of polyatomic molecules in degenerate electronic states I: orbital degeneracy. *Proc R Soc A* 161:220–235
- Kitagawa S, Okubo T, Kawata S, Kondo M, Katada M, Kobayashi H (1995) An oxalate-linked copper(II) coordination polymer, $[\text{Cu}_2(\text{oxalate})_2(\text{pyrazine})_3]_n$, constructed with two different copper units: X-ray crystallographic and electronic structures. *Inorg Chem* 34:4790–4796
- Lagier JP, Pezerat H, Dubernat J (1969) Magnesium, manganese, iron, cobalt, nickel, and zinc oxalate dihydrates. *Evolution*

- towards the best ordered form of compounds presenting stacking faults. *Rev Chim Miner* 6:1081–1093
- Libowitzky E (1999) Correlation of O–H stretching frequencies and O–H···O hydrogen bond lengths in minerals. *Monatsh Chem* 130:1047–1059
- Manasse E (1911) Oxalite (Humboldtine) from cape D’Arco (Elba). *Rend Accad Lincei* 19:138–145
- Matioli PA, Atencio D, Coutinho JMV, Menezes Filho LAD (1997) Humboldtina de Santa Maria de Itabira, Minas Gerais: primeira ocorrência brasileira e primeira ocorrência mundial em fraturas de pegmatito. *An Acad Bras Cienc* 69:431–432
- Mazzi F, Garavelli C (1957) Structure of oxalite, $\text{FeC}_2\text{O}_4 \cdot 2\text{H}_2\text{O}$. *Period Miner* 26:269–305
- Mazzi F, Garavelli CL (1959) Corrections of the structure of humboldtine (oxalite). *Period Mineral* 28:243–248
- Mikenda W (1986) Stretching frequency versus bond distance correlation of O–D(H)–Y (Y = N, O, S, Sc, Cl, Br, I) hydrogen bonds in solid hydrates. *J Mol Struct* 147:1–15
- Moore EA (2004) Metal-ligand bonding. Royal Society of Chemistry, Cambridge
- Nakamoto K (1997) Infrared and Raman spectra of inorganic and coordination compounds part A: theory and applications in inorganic chemistry. Wiley-Interscience, New York
- Nakamoto K, Margoshes M, Rundle RE (1955) Stretching frequencies as a function of distances in hydrogen bonds. *J Am Chem Soc* 77:6480–6486
- Novak A (1974) Hydrogen bonding in solids: correlation of spectroscopic and crystallographic data. *Struct Bond* 18:177–216
- Orgel LE, Dunitz JD (1957) Stereochemistry of cupric compounds. *Nature* 179:462–465
- Pezerat H, Dubernat J, Lagier JP (1968) Structure of magnesium, manganese, iron, cobalt, nickel, and zinc oxalate dihydrates. Existence of stacking faults. *C R Acad Sci Paris Ser C* 288:1357–1360
- Renner B, Lehmann G (1986) Correlation of angular and bond length distortions in TO_4 units in crystals. *Z Kristallogr* 175:43–59
- Shannon RD (1976) Revised effective ionic radii and synthetic studies of interatomic distances in halides and chalcogenides. *Acta Crystallogr A* 32:751–767
- Sheldrick GM (1997) SHELXL97. Program for refinement of crystal structures. University of Göttingen, Göttingen
- Silverstein RM, Bassler GC, Morrill TC (1991) Spectrometric identification of organic compounds, 5th edn. John Wiley, New York
- Śledzińska I, Murasik A, Piotrowski M (1986) Neutron diffraction study of crystal and magnetic structures of $\alpha\text{-FeC}_2\text{O}_4 \cdot 2\text{D}_2\text{O}$. *Physica B* 138:315–322
- Śledzińska I, Murasik A, Fischer P (1987) Magnetic ordering of the linear chain system manganese oxalate dehydrate investigated by means of neutron diffraction and bulk magnetic measurements. *J Phys C* 20:2247–2259
- Smith E, Dent G (2005) Modern Raman spectroscopy: a practical approach. John Wiley, New York
- Soleimannejad J, Aghabozorg H, Hooshmand S, Ghadermazi M, Gharamaleki JA (2007) The monoclinic polymorph of catena-poly [[diaquamanganese(II)]- μ -oxalate- $\kappa^4\text{O}^1, \text{O}^2: \text{O}^1', \text{O}^2'$] *Acta Crystallogr E* 63:m2389–m2390
- Stiefel EI, Brown GF (1972) Detailed nature of the six-coordinate polyhedra in tris (bidentate ligand) complexes. *Inorg Chem* 11:434–436
- Wilson MJ, Jones D (1984) The occurrence and significance of manganese oxalate in *Pertusaria corallina* (Lichenes). *Pedobiologia* 26:373–379